

# Each GPI-anchored protein species forms a specific lipid raft depending on its GPI attachment signal

Arisa Miyagawa-Yamaguchi<sup>1</sup> · Norihiro Kotani<sup>2</sup> · Koichi Honke<sup>1,3</sup>

Received: 26 February 2015 / Revised: 15 April 2015 / Accepted: 23 April 2015 / Published online: 7 May 2015  
© Springer Science+Business Media New York 2015

**Abstract** We previously reported a method, termed enzyme-mediated activation of radical sources (EMARS) for analysis of co-clustered molecules with horseradish peroxidase (HRP) fusion proteins expressed in living cells. This method is featured by radical formation of labeling reagents by HRP. In the current study, we have employed another labeling reagent, fluorescein-conjugated tyramide (FT) instead of the original arylazide compounds. Although hydrogen peroxide is required for the activation of FT, the labeling efficiency by HRP and the nonspecific reactions by endogenous enzyme(s) have been dramatically improved compared with the original fluorescein arylazide. This revised EMARS method has enabled visualization of co-clustered molecules in the endoplasmic reticulum and Golgi membranes with confocal microscopy. By using this method, we have found that GPI-anchored proteins, decay accelerating factor (DAF) and Thy-1 are exclusively co-clustered with HRP-DAFGPI and HRP-Thy1GPI, in which GPI attachment signals of DAF and Thy-1 have been connected to HRP, respectively. Furthermore, the *N*-glycosylation types of DAF and Thy-1 have been found to correspond to those of HRP-DAFGPI and HRP-Thy1GPI, respectively. These results indicate that each GPI-anchored protein species forms a specific lipid raft depending

on its GPI attachment signal, and that the EMARS method can segregate individual lipid rafts.

**Keywords** EMARS · HRP · Fluorescein tyramide · Visualization of co-clustering molecules · *N*-glycosylation

## Introduction

Lipid rafts are membrane microdomains formed by self-organization of cholesterol, (glyco)sphingolipids, glycosylphosphatidylinositol (GPI)-anchored proteins, Src-family kinases, and other membrane proteins [1–3]. Lipid rafts serve as a platform in a wide range of important biological events such as signal transduction, cell adhesion, migration, and protein trafficking [4–7]. To elucidate the molecular mechanisms of these events, identification of co-clustered molecules in individual raft domains is required.

Cholesterol is synthesized in the endoplasmic reticulum (ER) and the biosynthesis of (glyco)sphingolipids is carried out in the ER through the Golgi apparatus. Cholesterol-(glyco)sphingolipid rafts are assumed to assemble in the Golgi [4]. The inclusion of proteins into the rafts is important for their polarized delivery to the plasma membrane and the cluster formation with their coworkers. However, when and where raft components are incorporated remain unclear. It also remains to be elucidated how heterogeneous rafts are formed.

In a preceding study, we demonstrated that two kinds of GPI-anchored horseradish peroxidases (HRP-GPIs), in which GPI attachment signals of human decay accelerating factor (DAF) and Thy-1 are separately linked to the C-terminus of HRP, undergo different *N*-glycosylation and form distinct molecular clusters in the plasma membrane [8]. The difference in the *N*-glycan types implies that incorporation of GPI-anchored

✉ Koichi Honke  
khonke@kochi-u.ac.jp

<sup>1</sup> Center for Innovate and Translational Medicine, Kochi University Medical School, Nankoku, Kochi 783-8505, Japan

<sup>2</sup> Department of Biochemistry, Saitama Medical University, Iruma-gun, Saitama 350-0495, Japan

<sup>3</sup> Department of Biochemistry, Kochi University Medical School, Nankoku, Kochi 783-8505, Japan

proteins into a particular lipid raft occurs in the early stage of intracellular trafficking, before the processing of *N*-glycans [8, 9].

In that study [8], cluster formation was analyzed by a method termed enzyme mediated activation of radical sources (EMARS), which is featured by radical formation of labeling reagents by HRP [10–13]. The radicals produced by the EMARS reaction attack and make a covalent bond to the molecules in the vicinity within 300 nm from the HRP set on the probed molecule. Co-clustered molecules with the target molecule on which HRP is set are, thereby, labeled with the tag conjugated with radical sources. Originally, we have used arylazide-containing reagents as the labeling reagent [10–13]. However, their labeling efficiency is low, and non-specific reactions by endogenous enzyme(s) are of problem [10, 11].

In order to solve the problem, we have surveyed labeling reagents and found that fluorescein-conjugated tyramide (FT), in which arylazide is replaced with tyramide, is suitable for this use. Tyramide is converted to phenoxy radical by HRP in the presence of hydrogen peroxide, which covalently binds to tyrosine residues of proteins at or near the site of HRP activity [14] (Fig. 1). This reaction constitutes the basis of the well-known tyramide signal amplification (TSA) method for immunohistochemical staining [15] and is utilized for proteomic mapping of mitochondria composition in living cells [16]. However, it has never been applied to analysis of co-clustered molecules in lipid rafts.

By using the new EMARS system using FT as the labeling reagent, we investigated the issue of whether DAF and Thy-1 are co-clustered with the corresponding HRP-GPIs with the same GPI attachment signal. Moreover, we show that the revised EMARS method is applicable to analysis of co-clustered molecules in the intracellular organelles, the ER and the Golgi membranes.

## Material and methods

### Cell culture

HeLa (RIKEN Cell Bank) cells were cultured in D-MEM supplemented with 10 % fetal bovine serum (FBS) at 37 °C under humidified air containing 5 % CO<sub>2</sub>. A previously constructed HeLa S3-TetON/HRP-DAFGPI and HeLa S3-TetON/HRP-Thy1GPI cells [8] were cultured in RPMI 1640 medium.

### Vectors and transfection

We generated three types of expression constructs that contain HRP: constructs that express proteins targeted to endoplasmic reticulum (ER), Golgi and plasma membrane. The DNA

fragment encoding the mature region of *Armoracia rusticana* HRP (from Gln<sup>31</sup> to Ser<sup>338</sup>) was amplified from the *prxC1a* gene [17] by PCR. To generate an ER-targeted HRP construct, the ER retention signal, Lys-Asp-Glu-Leu (KDEL) was added to the C terminus of HRP. The HRP-KDEL fragment was subcloned into the *EcoRV* site of pSecTagA (Invitrogen). The Ig  $\kappa$ -chain leader sequence of pSecTagA was used as the *N*-terminal signal sequence in Ig $\kappa$ S-HRP-KDEL. The pmTurquoise2-Golgi (Addgene, number 36205) was used for generation of a Golgi-targeted HRP construct. The HRP fragment was subcloned into *Bam*HI site of pmTurquoise2-Golgi, resulting  $\beta$ 1,4-galactosyltransferase1 ( $\beta$ 4GalT1)-HRP. These plasmid DNAs were transfected into HeLa cells with Lipofectamine 2000 transfection reagent (Invitrogen) and transiently expressed. For plasma membrane-targeted HRP, GPI-anchored HRP (HRP-GPIs) were used as described previously [8]. The *N*-terminal signal peptide and the C-terminal GPI attachment signal of DAF and Thy-1 were connected to the corresponding terminus of HRP. The resulting HRP-DAFGPI and HRP-Thy1GPI fusion proteins were stably expressed in HeLa S3 cells by using a conditional expression system requiring doxycycline [8]. For the expression of HRP, the cells were incubated with the complete medium supplemented with 1 mg/ml doxycycline for 24 h.

### Synthesis of fluorescein-conjugated tyramide

100 mg of tyramine (Sigma) dissolved in 5 mL *N,N*-dimethylacetamide (DMAA) was added to 100 mg NHS-fluorescein (Thermo) in 5 mL DMAA. The mixture was incubated at room temperature for 12 h in dark. An aliquot of the mixture was applied to thin-layer chromatography (chloroform:methanol:water = 65:25:4 vol/vol) to check whether NHS-fluorescein was completely consumed. To remove excess tyramine, the mixture was applied to 8 mL of cation-exchange resin, AG-50WX8 (Bio-Rad) equilibrated with DMAA. An aliquot of the flow-through fraction was applied to thin-layer chromatography again to check whether tyramine was completely removed. The flow-through fraction containing fluorescein-conjugated tyramine (FT) was stored at –20 °C.

### EMARS reaction

The EMARS reaction and detection of EMARS products were performed as described previously [10, 13]. The cultured cells were incubated with 0.1 mM fluorescein-conjugated arylazide (FA) in PBS at room temperature for 15 min in dark. Otherwise fluorescein-conjugated tyramide (FT) was added in the cell culture media and the cells were incubated for 30 min at 37 °C. Then 1 mM H<sub>2</sub>O<sub>2</sub> was added for 5 min. After washing twice with PBS, the treated cells were collected into a plastic tube with 10 mM sodium azide in PBS. The cell suspension

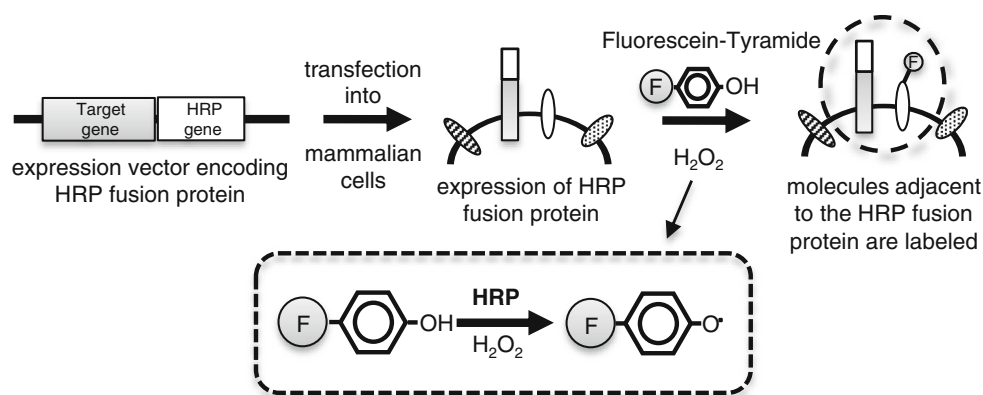


**Fig. 1** The labeling scheme using fluorescein-tyramide and expressed HRP. An expression vector encoding an HRP fusion protein is transfected into mammalian cells. Cells expressing an HRP fusion protein are supplemented with fluorescein-conjugated tyramide (FT) and  $\text{H}_2\text{O}_2$  to initiate the EMARS reaction. After EMARS reaction,

membrane proteins are solubilized and the fluorescein-labeled proteins are analyzed using a fluorescence imager. The phenoxyl radical that is generated by HRP is short-lived and covalently binds to neighboring proteins

was then homogenized through a syringe needle to break the plasma membranes and centrifuged at 800 g for 5 min. The supernatant was subsequently centrifuged at 20,000 g for 15 min to precipitate the plasma membrane fractions. After solubilization with the NP-40 lysis buffer (20 mM Tris-HCl, pH 7.4, 150 mM NaCl, 5 mM EDTA, 1 % NP-40, 1 % glycerol), the samples were subjected to SDS-PAGE (10 % gel), and were subsequently analyzed using LAS-4000 Bio-imaging analyzer (Fuji Film) equipped with blue light and Y515-Di filter under fluorescence mode for FA or FT detection.

### Confocal microscopy

Cells labeled as above were washed 3 times with PBS, then fixed with 7.4 % formaldehyde-PBS solution at room temperature for 10 min. Cells were then washed three times with PBS and permeabilized with 0.01 % Triton-X at room temperature for 10 min. For the confocal microscopy analysis of the expression and localization of HRP, cells were treated with antibodies against HRP (Jackson ImmunoResearch), Calnexin and GM130 at room temperature for 20 min. Then, the cells were treated with Alexa 594-conjugated anti-goat IgG antibody (Invitrogen) for HRP, Alexa 647-conjugated anti-mouse IgG antibody for Calnexin and Alexa 633-conjugated anti-mouse IgG antibody for GM130 at room temperature for 20 min. The cells were gently washed with PBS, and observed with confocal laser scan microscopy (FLUOVIEW FV1000, OLYMPUS).

### RTKs array analysis

A total of 20  $\mu\text{g}$  of the EMARS products were applied to a Proteome Profiler Human Phospho-RTK array (R&D Systems) following the manufactures instrument. After washing, the array was stained with HRP-conjugated anti-fluorescein antibody (0.1 mg/ml) and developed with an Immobilon

Western Chemi- luminescent HRP Substrate (Millipore). The detailed array coordinates were shown in the manufacture web page (<http://www.mdsystems.com/pdf/ary001b.pdf>).

### Enrichment of fluorescein-labeled EMARS products

The human Thy-1 (Gene No. KIEE0419) construct was created by transferring the coding sequences from the pF1KE0419 Flexi Vector (Kazusa DNA Research Institute) to pF5A CMV-neo Flexi Vector (Promega). The resulting vector, pThy-1, was constructed with the Flexi Vector System (Promega), a directional cloning method that shuttles protein-coding sequences between compatible vectors. HeLa S3 TetOn/HRP-DAFGPI and HeLa S3 TetOn/HRP-Thy1GPI cells were transfected with the human Thy-1 using MultiFectam (Promega). Four to six hours after transfection in Opti-MEM (Invitrogen), the cell culture medium was changed back to complete media supplemented with or without 1 mg/ml doxycycline. Twenty-four hours after media change, the EMARS reaction was performed using FT as described above. The microsome fraction was obtained from the cell lysates and washed with 10 mM sodium azide. The resulting pellet was suspended in 500  $\mu\text{L}$  of chloroform:methanol (2:1 by volume). After addition of 500  $\mu\text{L}$  of deionized water, sample was gently agitated and centrifuged at 10,000 $\times g$  for 5 min. All the solvent was removed, 500  $\mu\text{L}$  of 50 % methanol was added to the pellet. After gentle agitation, the solvent was removed. The wash with 50 % methanol was repeated until excess FT was completely removed. After evaporation, 100  $\mu\text{L}$  of 50 mM Tris-HCl (pH 7.4) containing 1 % SDS was added, and then heated at 100  $^{\circ}\text{C}$  for 10 min. The soluble material was transferred into a new tube and then diluted with 400  $\mu\text{L}$  of NP-40 lysis buffer. Then, we tried to purify and concentrate fluorescein-labeled proteins as described previously [13].

Twenty microliters of prepared anti-fluorescein antibody Sepharose was added to the sample, and mixed with rotation at 4 °C for overnight. The treated Sepharose were washed with NP-40 lysis buffer five times, PBS containing 0.5 M NaCl twice and distilled water once. The adsorbed fluorescein-tagged molecules were eluted with SDS-PAGE sample buffer at 100 °C for 5 min. The elute was subjected to SDS-PAGE (15 % gel). After electrophoresis, the gel was analyzed using LAS-4000 as described above.

### Glycosidase treatment

Cell lysates were deglycosylated by Peptide-N4-(N-acetyl- $\beta$ -glucosaminyl)asparagine amidase F (PNGase) (Sigma-Aldrich), endo- $\beta$ -N-acetylglucosaminidase H (EndoH) (New England Bio-labs) or sialidase (Roche Applied Science) treatment. Lysates were incubated with 10 % (vol/vol) denaturing buffer (5 % SDS, 0.4 M DTT) at 100 °C for 10 min. The deglycosylation was performed using 0.1 U/ml PNGaseF, 50 U/ml EndoH, or 0.002 U/ml sialidase in the presence of 10 % (vol/vol) NP-40 and 50 mM sodium phosphate, pH 7.5 for PNGase, 50 mM sodium citrate, pH 5.5 for EndoH, or pH 4.5 for sialidase, at 37 °C overnight.

### Western blots

Following the EMARS reaction in HeLa S3 cells, microsome lysate was applied to immunoaffinity chromatography with anti-fluorescein antibody Sepharose as described above. The adsorbed beads were treated with SDS sample buffer at 100 °C for 5 min, and the eluted samples were, respectively, subjected to SDS-PAGE (15 % gel) under reducing condition. After blotting onto a PVDF membrane, the membrane was treated with anti-bodies: anti-CD55 mouse antibody (1:200; Ancell), anti-Thy-1 mouse antibody (1:500; Abcam) and anti-HRP goat antibody (1:5000; Jackson ImmunoResearch). Then, the membranes were reacted with HRP-conjugated anti-mouse IgG antibody (1:50000; Promega) and HRP-conjugated anti-goat IgG antibody (1:10000; Promega).

## Results

### The new EMARS system using fluorescein tyramide (FT) as the labeling reagent

In order to modify the original labeling reagent, fluorescein arylazide (FA), fluorescein tyramide (FT) was constructed by condensation reaction of NHS-fluorescein and tyramine. For comparison of the performance between FA and FT, the EMARS reaction was performed using the expressed HRP-DAFGPI in HeLaS3 cells [8]. In the case of FT, 1 mM H<sub>2</sub>O<sub>2</sub> was added to the cell medium. The fluorescein-tagged

proteins resulting from the EMARS reaction were subjected to SDS-PAGE, and then detected directly with an LAS-4000 fluorescence imaging system. As a result, much more intense labeling was observed when FT was used in the EMARS reaction (Fig. 2a, + lanes) and nonspecific labeling by endogenous enzymes was hardly detected with FT (Fig. 2a, – lanes) as compared with FA. Cytochemical imaging with a confocal microscopy showed that the cell surface was labeled by fluorescein in both cases of FA and FT, but much more intense signal was gained by using FT compared with FA (Fig. 2b). Fluorescein-labeled molecules by the EMARS reaction with FA and FT were compared using a receptor tyrosine kinases (RTKs) antibody array, which consists of 94 spots of antibodies against 42 kinds of RTKs and control antibodies in duplicate. Although there was a marked difference in the labeling efficiency (Fig. 2a), the pattern of labeled RTKs was quite similar between FA and FT (Fig. 2c), indicating that FA and FT work in a similar way. These results demonstrated that FT is a better labeling reagent for the EMARS reaction than the original FA.

### The EMARS system with FT is applicable to visualization of co-clustered molecules in the intracellular organelles

Since we noticed that FT shows a high efficiency, preventing from activation by endogenous enzymes, we investigated the issue of whether FT is applicable to analysis of co-clustered molecules in the intracellular organelles. To this end, we constructed HRPs targeted to the ER and the Golgi. To localize it in the ER, the ER retention sequence, KDEL, was added to the C terminal of HRP (HRP-KDEL). As shown in Fig. 3a, The expressed HRP-KDEL detected with an anti-HRP antibody was co-localized with an ER marker, calnexin (*Calnexin/HRP*) and fluorescein labeling resulting from the EMARS reaction was also co-localized with the HRP-KDEL (*Fluorescein/HRP*). We generated a Golgi-targeted HRP construct by fusing the cDNAs of a Golgi-resident enzyme,  $\beta$ 1,4-galactosyltransferase1 and HRP ( $\beta$ 4GalT1-HRP). The expressed  $\beta$ 4GalT1-HRP detected with an anti-HRP antibody was co-localized with a Golgi marker, GM130 (Fig. 3b, *GM130/HRP*) and fluorescein labeling resulting from the EMARS reaction was co-localized with the  $\beta$ 4GalT1-HRP (Fig. 3b, *Fluorescein/HRP*). These observations indicate that the EMARS reaction with FT as the labeling reagent is applicable to the analysis of co-clustered molecules in the intracellular organelles.

### GPI-anchored proteins are exclusively co-clustered with the corresponding HRP-GPIs that have identical GPI attachment signals

We previously demonstrated by using the EMARS method that two kinds of GPI-anchored HRPs with different GPI



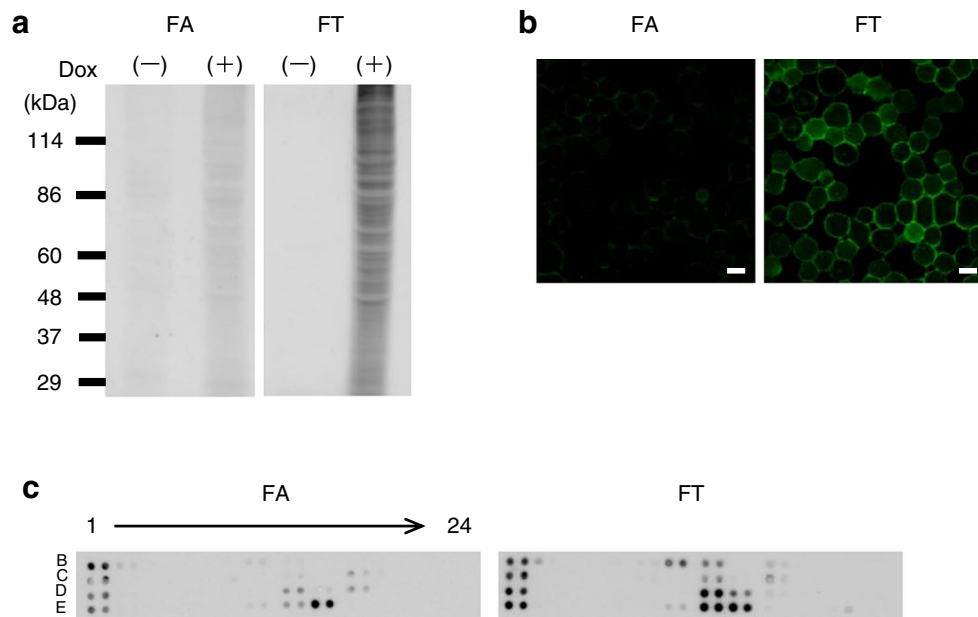


**Fig. 2** Comparison of fluorescein labeling between FA and FT. The EMARS reaction was performed using FA or FT as a labeling reagent in the HRP-DAFGPI-introduced cells that had been incubated with (+) or without (–) doxycycline. After the EMARS reaction, (a) 10 µg of microsome proteins were subjected to SDS-PAGE and analyzed by a LAS-4000 fluorescence imager, (b) the cells were fixed and analyzed for fluorescein by confocal laser scan microscopy. Bars=10 µm. c Identification of the fluorescein-labeled EMARS products by the

antibody array analysis. HeLa S3 cells that express HRP-DAFGPI were subjected to the EMARS reaction with FA or FT. Cell membrane extracts (20 µg total protein) were applied to a RTKs antibody array and the EMARS reaction products were detected with an anti-fluorescein antibody. The detailed array coordinates are shown in the manufacture web page (R&D Systems, Human Phospho-RTK Array, <http://www.rndsystems.com/pdf/ary001b.pdf>)

attachment signals derived from human DAF and Thy-1, HRP-DAFGPI and HRP-Thy1GPI form distinct clusters [8]. In the current study, we investigated the issue of whether DAF and Thy-1 are included in the clusters of HRP-DAFGPI and HRP-Thy1GPI, respectively. First, cDNA of human Thy-1 was separately transfected into HeLaS3/DAF-HRP-GPI and HeLaS3/Thy-1GPI cells, because Thy-1 was not expressed in HeLaS3 cells although DAF was endogenously expressed. By Western blot analysis with an anti-DAF antibody, endogenous DAF was detected at 86 kDa (Fig. 4a, control and *pThy-1*). After transfection with *Thy-1* cDNA, Thy-1 protein emerged at 22 kDa (Fig. 4a, *pThy-1*). Thus, we established HeLaS3/DAF-HRP-GPI and HeLaS3/Thy-1GPI cells that express both of DAF and Thy-1. Then, we performed the EMARS reaction with FT in the Thy-1-introduced HeLaS3/DAF-HRP-GPI and HeLaS3/Thy-1GPI cells. The fluorescein-labeled EMARS products were purified and concentrated by immunoaffinity chromatography using anti-fluorescein antibody-immobilized Sepharose. The unreacted FT was removed by solvent extraction before the immunoaffinity chromatography to prevent its interruption in the binding of fluorescein-labeled EMARS products to the immobilized anti-fluorescein antibody. As shown in Fig. 4b, fluorescein-labeled molecules were certainly concentrated by the immunoaffinity chromatography (compare lanes of *Input* and *IP*). The EMARS reaction mixture before the immunoaffinity chromatography (*Input*) and the

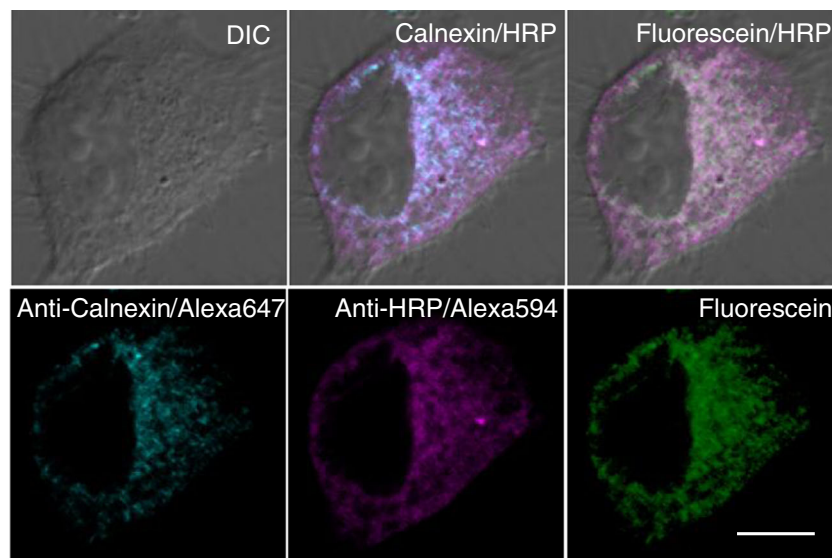
eluate fraction (*IP*) were separately subjected to Western blotting using antibodies against DAF and Thy-1 (Fig. 4c, upper panels). Although both samples with and without doxycycline contained the same amount of DAF and Thy-1 before immunoaffinity chromatography (Fig. 4c, *Input*), fluorescein-labeled DAF and Thy-1 were only detected in the cells with doxycycline (Fig. 4c, *IP*), indicating that these proteins are labeled with fluorescein by the EMARS reaction, depending on the expressed HRP (Fig. 4c, lower panels). Interestingly, the intensity of fluorescein-labeled DAF was more robust than that of Thy-1 in HeLaS3/HRP-DAFGPI cells (Fig. 4c, upper panels, HRP-DAFGPI, *IP*, (+) lane), whereas the intensity of fluorescein-labeled Thy-1 was stronger than that of DAF (Fig. 4c, upper panels, HRP-Thy1GPI, *IP*, (+) lane). In addition, HRP-DAFGPI and HRP-Thy1GPI were labeled with fluorescein by the EMARS reaction of themselves (Fig. 4c, lower panels). These results indicate that DAF and Thy-1 are exclusively co-clustered with HRP-DAFGPI and HRP-Thy1GPI, respectively.

#### GPI-anchored proteins have the same type of *N*-glycan as the corresponding HRP-GPIs that have identical GPI attachment signals

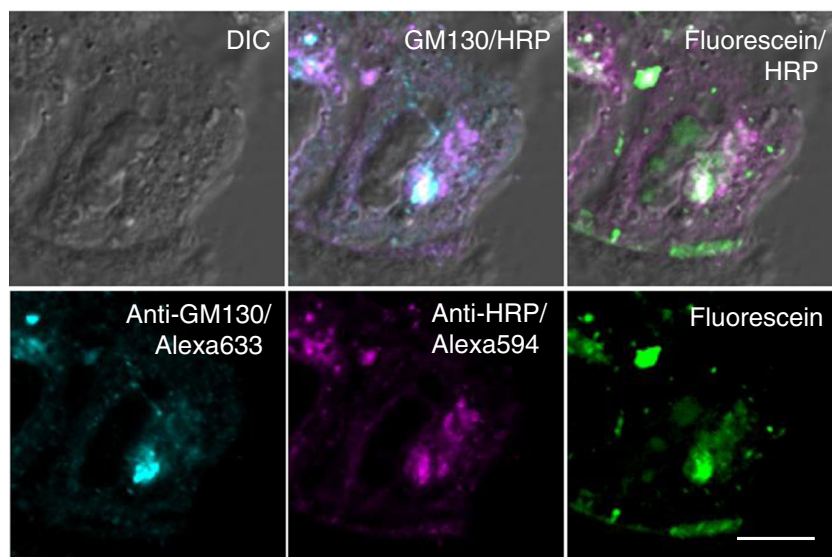
In the previous study [8], we found that HRP-DAFGPI has complex type *N*-glycans, while HRP-Thy1GPI carries high

**Fig. 3** Imaging analysis of fluorescein labeling by the EMARS reaction using the HRP's expressed in the ER and Golgi membranes. HeLa cells were separately transfected with the HRP constructs targeted to the ER (**a**, HRP-KDEL) and the Golgi (**b**,  $\beta$ 4GalT1-HRP). Following the EMARS reaction with FT and  $H_2O_2$ , cells were stained for the expressed HRP proteins with an anti-HRP antibody and an Alexa594-conjugated second antibody (**a** and **b**); for an ER marker, calnexin with an anti-calnexin and an Alexa647-conjugated second antibody (**a**); and for a *trans* Golgi marker, GM130 with anti-GM130 antibody and Alexa633-conjugated second antibody (**b**). After staining, cells were observed by confocal microscopy. All scale bars = 10  $\mu$ m

### a HRP-KDEL



### b $\beta$ 4GalT1-HRP



mannose type *N*-glycans, indicating that HRP-DAFGPI and HRP-Thy1GPI undergo different glycosylation in spite of the sameness of the peptide moiety except for the C-terminal attachment signals [9]. This phenomenon prompted us to elucidate which types of *N*-glycans are attached to DAF and Thy1 in HeLaS3 cells. As shown in the *upper panel* of Fig. 5, the 86 kDa molecule of DAF was resistant to EndoH, but sensitive to sialidase in both of the HRP-DAFGPI and HRP-Thy1GPI-expressing HeLa S3 cells. By contrast, the 22 kDa molecule of Thy-1 was EndoH-sensitive but sialidase-resistant in both the cells (Fig. 5, *lower panel*). These results indicate that the *N*-glycosylation types of DAF and Thy-1 correspond to that of HRP-DAFGPI and HRP-Thy1GPI,

respectively, and suggests that DAF and HRP-DAFGPI undergo the same process of *N*-glycosylation and so do Thy-1 and HRP-Thy1GPI.

### Discussion

The EMARS system is a comprehensive approach to identify interactions of cell-surface molecules under living conditions [10–13]. However, number of molecules labeled by the EMARS reaction are very small since the radical formation activity of HRP from arylazide compounds is weak. To make the EMARS method a powerful tool for a wide range of

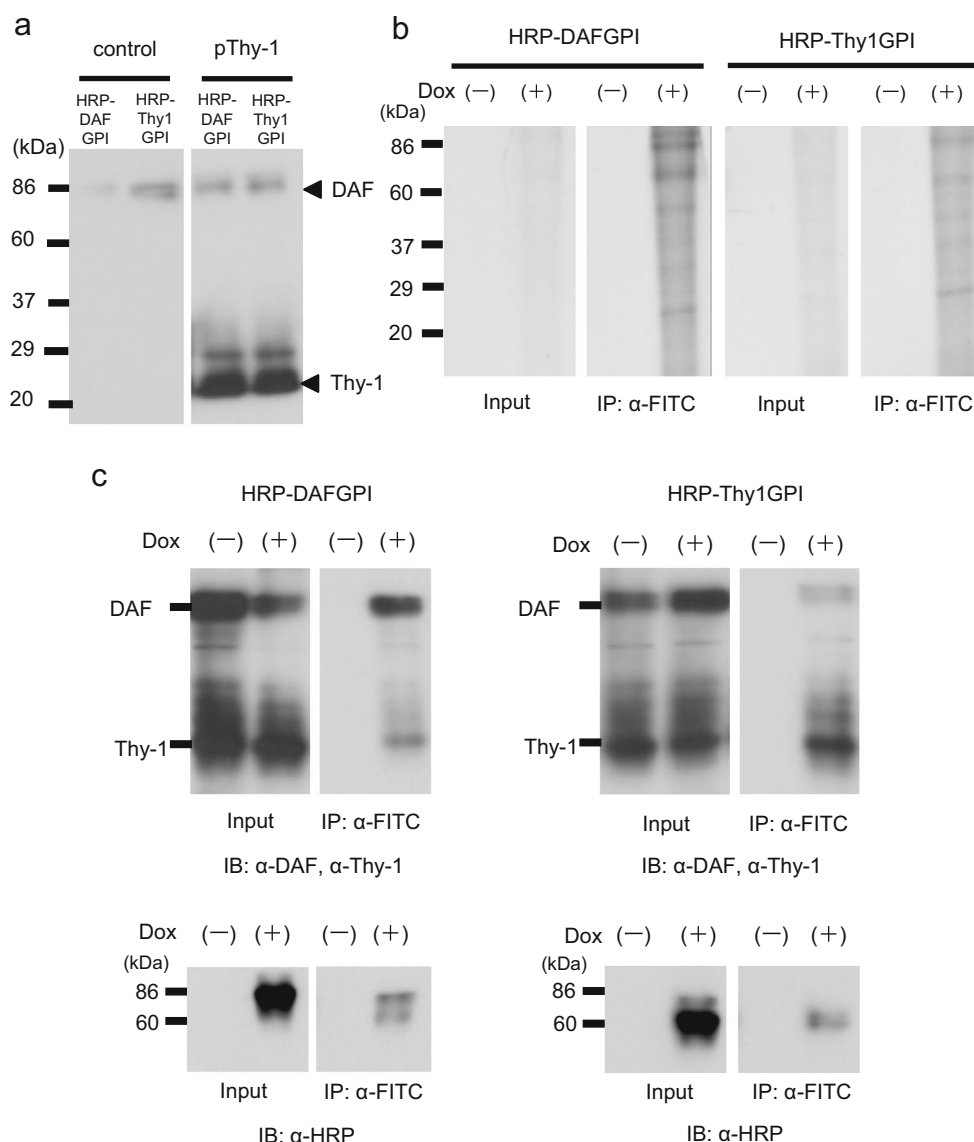


**Fig. 4** DAF and Thy-1 co-clustered with HRP-DAFGPI and HRP-Thy1GPI. **a** Expression of DAF and Thy-1 in the HRP-DAFGPI or HRP-Thy1GPI-introduced HeLa S3 cells. Cells were untransfected (control) or transfected with pThy-1, and analyzed for DAF and Thy-1 by Western blotting with an anti-DAF and anti-Thy-1 antibody. **b** Purification and concentration of fluorescein-labeled molecules. The HRP-DAFGPI or HRP-Thy1GPI-introduced HeLa S3 cells, in which pThy-1 had been transfected were cultured with (+) or without (-) doxycycline. Following the EMARS reaction with FT, the cells were solubilized and applied to immunoaffinity chromatography. The eluate

fraction (IP) was subjected to SDS-PAGE (15 % gel), and then analyzed with LAS-4000. The cell lysates before the immunoaffinity chromatography (input) were also applied to SDS-PAGE. **c** DAF, Thy-1 and HRP labeled by the EMARS reaction of HRP-DAFGPI or HRP-Thy1GPI. The EMARS products were applied to the immunoaffinity chromatography with anti-fluorescein antibody-immobilized Sepharose as described in (b). The eluate fraction (IP) and cell lysates before the immunoaffinity chromatography (input) were subjected to Western blotting with an anti-DAF, anti-Thy-1 and anti-HRP antibody

research concerning molecular interactions, the labeling efficiency must be improved. The present study is undertaken to establish such an efficient EMARS method. Tyramide compounds such as FT have two advantages for this purpose. First, the labeling efficiency of FT is much higher than that of the original arylazide conjugate, FA. Secondly, when FT is used as a labeling reagent, nonspecific labeling by endogenous enzyme(s) is remarkably reduced compared with FA. The superiority of the revised EMARS method enabled

analysis of co-clustered molecules in the intracellular organelles such as the ER and the Golgi membranes. In the present study, peroxidase activity of the expressed HRP was preserved in the ER and the Golgi, being consistent with the report that HRP expressed in the ER and the Golgi can be used for electron microscopy technology as a genetic tag [18].

In the original EMARS method [10], arylazide is converted to nitrene radical by HRP in the absence of hydrogen peroxide. The catalytic site of HRP may be different from that of the

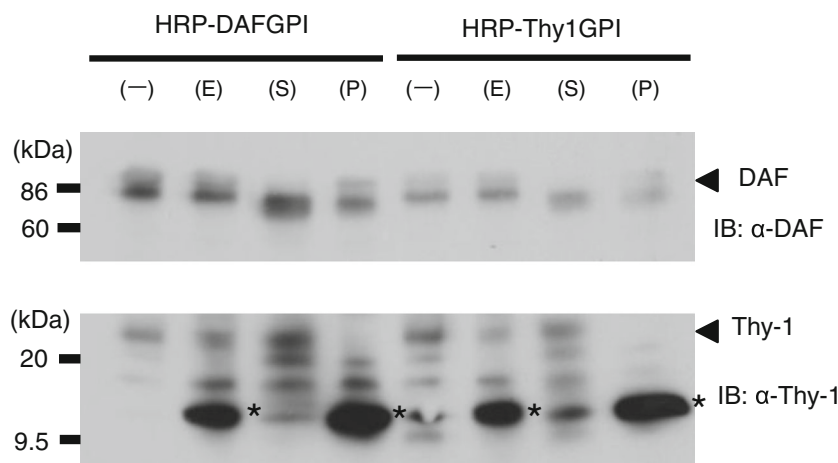


**Fig. 5** Difference in *N*-glycosylation between DAF and Thy-1. The HRP-DAFGPI or HRP-Thy1GPI-introduced HeLa S3 cells, in which pThy-1 had been transfected were cultured with doxycycline. The cell lysates were untreated (–) or treated with EndoH (*E*), sialidase (*S*), or PNGase (*P*) and subsequently analyzed by Western blotting with an

anti-DAF and anti-Thy-1 antibody. The original positions of DAF and Thy-1 are indicated on the right side. Note that the reactivity with anti-Thy-1 antibody is enhanced after removal of *N*-glycans in the lanes of (*E*) and (*P*) (asterisks)

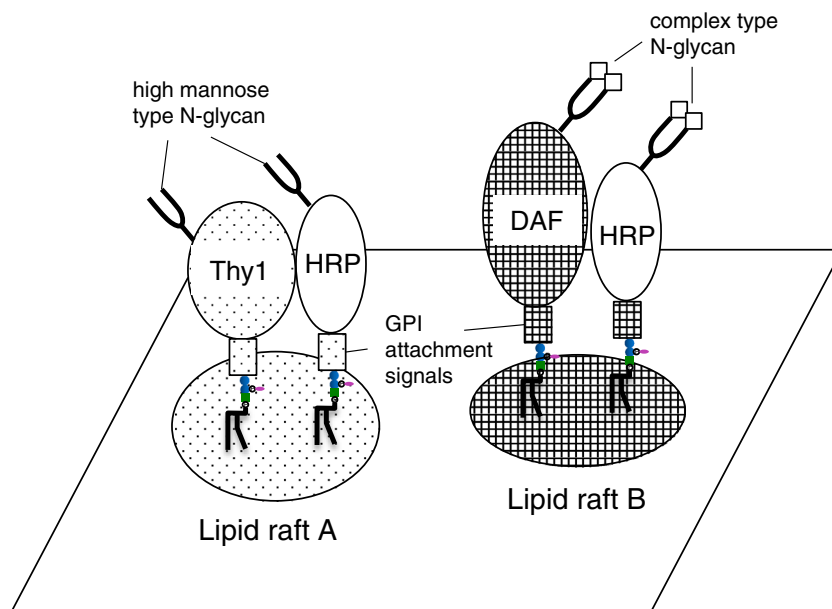
peroxidase activity, because the EMARS reaction with arylazide compounds does not need hydrogen peroxide and does not inhibit the peroxidase activity (data not shown). In contrast to this, tyramide is converted to phenoxy radical in the presence of hydrogen peroxide by the peroxidase activity of HRP [14]. Preliminary study indicated that 1 mM hydrogen peroxide is sufficient for the EMARS reaction. We were concerned about influence of hydrogen peroxide on cell viability, but there was no apparent difference in cell survival and morphology under 1 mM  $H_2O_2$  for a short period of 5 min (data not shown for cell survival). It was reported that the extracellular signal-regulated kinases (ERKs) begin to be activated from 5 min after addition of 1 mM  $H_2O_2$  in cardiac myocytes

[19], although  $H_2O_2$  is relatively stable among reactive oxygen species.

The phenoxyl radicals are also short lived and have a small labeling radius (<20 nm) [20] compared with nitrene radicals (<300 nm) [10]. Judging from the result of antibody microarray (Fig. 2c), in which similar proteins were labeled by the EMARS reaction with FT and FA, their labeling radius may be close in the situation of living cells.

In mammalian cells, more than 150 membrane proteins are GPI-anchored [21]. GPI is transferred by GPI transamidase to proteins that have a GPI attachment signal sequence at their C-termini in the ER [22]. The GPI attachment signals are poorly conserved on the sequence level, but are composed of four

**Fig. 6** Schematic presentation of GPI attachment signal-dependent lipid raft formation





regions: a linker region of about 10 amino acid residues upstream the cleavage site ( $\omega$  site), a region of small residues ( $\omega - 1$  to  $\omega + 2$ ) including the GPI-attachment site, a short stretch of hydrophilic amino acids, and the C-terminal hydrophobic tail [23]. It is reported that GPI-anchored GFP fusion proteins having distinct GPI attachment signals are differently sorted depending on their ability of oligomerization [24]. In the preceding study [8], we presented evidence that GPI-anchored HRP fusion proteins with different GPI attachment signals, HRP-DAFGPI and HRP-Thy1GPI undergo different *N*-glycosylation and form distinct clusters. The fact that inhibition of the *N*-glycosylation processing in the Golgi did not influence on their cluster formation suggests that lipid raft formation of HRP-GPIs initiates in the early stage of intracellular trafficking, prior to the *N*-glycosylation processing [8, 9]. In addition to these findings, we have found in the current study that DAF and Thy-1 are exclusively co-clustered with HRP-DAFGPI and HRP-Thy1GPI, respectively (schematically shown in Fig. 6), and also possess an identical type of *N*-glycans with HRP-DAFGPI and HRP-Thy1GPI, respectively (also shown in Fig. 6). These results indicate that DAF and Thy-1 are included in distinct lipid rafts and differently delivered to the plasma membrane through distinct routes in the Golgi.

GPI-anchored proteins are considered to interact with other molecules in lipid rafts via the GPI moiety and/or the protein ectodomain [24]. Our results indicate that cluster formation of GPI-anchored proteins is dependent on the GPI attachment signal sequence. Only three amino acids ( $\omega - 2$  to  $\omega$ ) in the proximal linker region are responsible for the cluster formation [8]. Paradino *et al.* [24] assume that differences in the GPI moiety are responsible for the different sorting of GPI-anchored GFP fusion proteins because only two amino acids ( $\omega - 1$  and  $\omega$ ) are sufficient for the specific sorting. The proximal linker region might influence the remodeling of GPI anchors in the ER through the Golgi [25].

In the present study, human DAF and Thy-1 expressed in HeLa S3 cells have complex type and high mannose type *N*-glycans, respectively. There are reports on *N*-glycosylation of human DAF and Thy-1. One complex-type *N*-glycan chain is attached to Asn-63 of human DAF [26]. The DAF *N*-glycan is dispensable for complement regulation [27], but assumed to protect the protein from proteases [26]. Thy-1 is an immunoglobulin superfamily protein containing three *N*-glycosylation sites, one of which (Asn-23) is mainly occupied with oligomannose [28]. Devasahayam *et al.* [29] reported that the GPI-anchored form Thy-1 is less processed with more oligomannose than the soluble form Thy-1. The function of the Thy-1 *N*-glycan is unknown. These reports are consistent with the results in the current study.

In conclusion, we have established an efficient EMARS method using fluorescein-conjugated tyramide that is applicable to the analysis of co-clustered molecules in the

intracellular organelles as well as on the cell surface. By using this method, we found that GPI-anchored proteins are exclusively co-clustered with the corresponding HRP-GPIs that have the same GPI attachment signals. In addition, GPI-anchored proteins have an identical type of *N*-glycan with the corresponding HRP-GPIs that have the same GPI attachment signals. These results indicate that each GPI-anchored protein species forms a specific lipid raft depending on its GPI attachment signal, and that the EMARS method can segregate individual lipid rafts.

#### Compliance with ethical standard

**Conflict of interest** The authors declare that they have no conflict of interest.

**Ethical approval** This article does not contain any studies with human participants or animals performed by any of the authors.

#### References

1. Lingwood, D., Simons, K.: Lipid rafts as a membrane-organizing principle. *Science* **327**, 46–50 (2010). doi:10.1126/science.1174621
2. Kusumi, A., Fujiwara, T.K., Morone, N., Yoshida, K.J., Chadda, R., Xie, M., Kasai, R.S., Suzuki, K.G.N.: Membrane mechanisms for signal transduction: the coupling of the meso-scale raft domains to membrane-skeleton-induced compartments and dynamic protein complexes. *Semin. Cell Dev. Biol.* **23**, 126–144 (2012). doi:10.1016/j.semcdb.2012.01.018
3. Vereb, G., Szöllosi, J., Matkó, J., Nagy, P., Farkas, T., Vigh, L., Mátyus, L., Waldmann, T.A., Damjanovich, S.: Dynamic, yet structured: the cell membrane three decades after the Singer-Nicolson model. *Proc. Natl. Acad. Sci. U. S. A.* **100**, 8053–8058 (2003). doi:10.1073/pnas.1332550100
4. Brown, D.A., London, E.: Functions of lipid rafts in biological membranes. *Annu. Rev. Cell Dev. Biol.* **14**, 111–136 (1998). doi:10.1146/annurev.cellbio.14.1.111
5. Simons, K., Toomre, D.: Lipid rafts and signal transduction. *Nat. Rev. Mol. Cell Biol.* **1**, 31–39 (2000). doi:10.1126/science.1174621
6. Harris, T.J.C., Siu, C.H.: Reciprocal raft-receptor interactions and the assembly of adhesion complexes. *Bioessays* **24**, 996–1003 (2002). doi:10.1002/bies.10172
7. Tsui-Pierchala, B.A., Encinas, M., Milbrandt, J., Johnson, E.M.: Lipid rafts in neuronal signaling and function. *Trends Neurosci.* **25**, 412–417 (2002). doi:10.1016/S0166-2236(02)02215-4
8. Miyagawa-Yamaguchi, A., Kotani, N., Honke, K.: Expressed glycosylphosphatidylinositol-anchored horseradish peroxidase identifies co-clustering molecules in individual lipid raft domains. *PLoS ONE* **9**, e93054 (2014). doi:10.1371/journal.pone.0093054
9. Miyagawa-Yamaguchi, A., Kotani, N., Honke, K.: Segregation of lipid rafts revealed by the EMARS method using GPI-anchored HRP fusion proteins. *Trends. Glycosci. Glycotech.* **26**, 59–69 (2014). doi:10.4052/tigg.26.59
10. Kotani, N., Gu, J., Isaji, T., Udaka, K., Taniguchi, N., Honke, K.: Biochemical visualization of cell surface molecular clustering in living cells. *Proc. Natl. Acad. Sci. U. S. A.* **105**, 7405–7409 (2008). doi:10.1073/pnas.0710346105

11. Honke, K., Kotani, N.: The enzyme-mediated activation of radical source reaction: a new approach to identify partners of a given molecule in membrane microdomains. *J. Neurochem.* **116**, 690–695 (2011). doi:[10.1111/j.1471-4159.2010.07027.x](https://doi.org/10.1111/j.1471-4159.2010.07027.x)
12. Honke, K., Kotani, N.: Identification of cell-surface molecular interactions under living conditions by using the enzyme-mediated activation of radical sources (EMARS) method. *Sensors* **12**, 16037–16045 (2012). doi:[10.3390/s121216037](https://doi.org/10.3390/s121216037)
13. Jiang, S., Kotani, N., Ohnishi, T., Miyagawa-Yamaguchi, A., Tsuda, M., Yamashita, R., Ishiura, Y., Honke, K.: A proteomics approach to the cell-surface interactome using the enzyme-mediated activation of radical sources reaction. *Proteomics* **12**, 54–62 (2012). doi:[10.1002/pmic.201100551](https://doi.org/10.1002/pmic.201100551)
14. Bobrow, M.N., Harris, T.D., Shaughnessy, K.J., Litt, G.J.: Catalyzed reporter deposition, a novel method of signal amplification. Application to immunoassays. *J. Immunol. Methods* **125**, 279–285 (1989). doi:[10.1016/0022-1759\(89\)90104-X](https://doi.org/10.1016/0022-1759(89)90104-X)
15. Adams, J.C.: Biotin amplification of biotin and horseradish peroxidase signals in histochemical stains. *J. Histochem. Cytochem.* **40**, 1457–1463 (1992). doi:[10.1177/40.10.1527370](https://doi.org/10.1177/40.10.1527370)
16. Rhee, H.W., Zou, P., Udeshi, N.D., Martell, J.D., Mootha, V.K., Carr, S.A., Ting, A.Y.: Proteomic mapping of mitochondria in living cells *via* spatially restricted enzymatic tagging. *Science* **15**, 1328–1331 (2013). doi:[10.1126/science.1230593](https://doi.org/10.1126/science.1230593)
17. Matsui, T., Nakayama, H., Yoshida, K., Shinmyo, A.: Vesicular transport route of horseradish Cl<sub>a</sub> peroxidase is regulated by N- and C-terminal propeptides in tobacco cells. *Appl. Microbiol. Biotechnol.* **62**, 517–522 (2003). doi:[10.1007/s00253-003-1273-z](https://doi.org/10.1007/s00253-003-1273-z)
18. Schikorski, T.: Horseradish peroxidase as a reporter gene and as a cell-organelle-specific marker in correlative light-electron microscopy. *Methods Mol. Biol.* **657**, 315–327 (2010). doi:[10.1007/s00253-003-1273-z](https://doi.org/10.1007/s00253-003-1273-z)
19. Aikawa, R., Komuro, I., Yamazaki, T., Zou, Y., Kudoh, S., Tanaka, M., Shinojima, I., Hiroi, Y., Yazaki, Y.: Oxidative stress activates extracellular signal-regulated kinases through Src and Ras in cultured cardiac myocytes of neonatal rats. *J. Clin. Invest.* **100**, 1813–1821 (1997). doi:[10.1172/JCI119709](https://doi.org/10.1172/JCI119709)
20. Bendayan, M.: Worth its weight in gold. *Science* **291**, 1363–1365 (2001). doi:[10.1126/science.291.5507.1363](https://doi.org/10.1126/science.291.5507.1363)
21. Orlean, P., Menon, A.K.: Thematic review series: lipid posttranslational modifications. GPI anchoring of protein in yeast and mammalian cells, or: how we learned to stop worrying and love glycosphospholipids. *J. Lipid Res.* **48**, 993–1011 (2007). doi:[10.1194/jlr.R700002-JLR200](https://doi.org/10.1194/jlr.R700002-JLR200)
22. Chen, R., Knez, J.J., Merrick, W.C., Medof, M.E.: Comparative efficiencies of C-terminal signals of native glycosphosphatidylinositol (GPI)-anchored proteins in conferring GPI-anchoring. *J. Cell. Biochem.* **84**, 68–83 (2002). doi:[10.1002/jcb.1267](https://doi.org/10.1002/jcb.1267)
23. Eisenhaber, B., Bork, P., Eisenhaber, F.: Sequence properties of GPI-anchored proteins near the omega-site: constraints for the polypeptide binding site of the putative transamidase. *Protein Eng. Des. Sel.* **11**, 1155–1161 (1998). doi:[10.1093/Protein/11.12.1155](https://doi.org/10.1093/Protein/11.12.1155)
24. Paladino, S., Lebreton, S., Tivodar, S., Campana, V., Tempre, R., Zurzolo, C.: Different GPI-attachment signals affect the oligomerisation of GPI-anchored proteins and their apical sorting. *J. Cell Sci.* **121**, 4001–4007 (2008). doi:[10.1242/jcs.036038](https://doi.org/10.1242/jcs.036038)
25. Fujita, M., Kinoshita, T.: GPI-anchor remodeling: potential functions of GPI-anchors in intracellular trafficking and membrane dynamics. *Biochim. Biophys. Acta* **1821**, 1050–1058 (2012). doi:[10.1016/j.bbalip.2012.01.004](https://doi.org/10.1016/j.bbalip.2012.01.004)
26. Lukacik, P., Roversi, P., White, J., Esser, D., Smith, G.P., Billington, J., Williams, P.A., Rudd, P.M., Wormald, M.R., Harvey, D.J., Crispin, M.D.M., Radcliffe, C.M., Dwek, R.A., Evans, D.J., Morgan, B.P., Smith, R.A.G., Lea, S.M.: Complement regulation at the molecular level: the structure of decay-accelerating factor. *Proc. Natl. Acad. Sci. U. S. A.* **101**, 1279–1284 (2004). doi:[10.1073/pnas.0307200101](https://doi.org/10.1073/pnas.0307200101)
27. Brodbeck, W.G., Kuttner-Kondo, L., Mold, C., Medof, M.E.: Structure/function studies of human decay-accelerating factor. *Immunology* **101**, 104–111 (2000). doi:[10.1046/j.1365-2567.2000.00086.x](https://doi.org/10.1046/j.1365-2567.2000.00086.x)
28. Parekh, R.B., Tse, A.G., Dwek, R.A., Williams, A.F., Rademacher, T.W.: Tissue-specific N-glycosylation, site-specific oligosaccharide patterns and lentil lectin recognition of rat Thy-1. *EMBO J.* **6**, 1233–1244 (1987)
29. Devasahayam, M., Catalino, P.D., Rudd, P.M., Dwek, R.A., Barclay, A.N.: The glycan processing and site occupancy of recombinant Thy-1 is markedly affected by the presence of a glycosylphosphatidylinositol anchor. *Glycobiology* **9**, 1381–1387 (1999)